Inorg. Chem. **2008**, *47*, 10196−10198

Inorganic Chemistry

Communication

Remarkably Bent, Ethane-Linked, Diiron(III) μ-Oxobisporphyrin: Synthesis, Structure, Conformational Switching, and Photocatalytic Oxidation

Sudip Kumar Ghosh, Ranjan Patra, and Sankar Prasad Rath*

Department of Chemistry, Indian Institute of Technology Kanpur, Kanpur 208016, India

Received July 29, 2008

A remarkably bent diiron(III) μ-oxobisporphyrin containing a highly flexible ethane linker is reported that authenticates, for the first time, the unprecedented ability of this platform to “open” and “close” its binding pockets, leading to facile syn−anti conformational switching with very high vertical flexibility of over 6.5 Å in a single molecular framework. X-ray structural characterization reveals the bent diiron(III) μ-oxobisporphyrins with the smallest known Fe−O−Fe angles of 147.9(1)° for any iron(III) μ-oxo porphyrin dimers reported so far. Two rings in a molecule are not slipped but are face to face in a nearly eclipsed geometry and are placed so close that at least six carbon atoms from each of the macrocycles are driven to be essentially less than the van der Waals contacts (<3.4 Å). The complex catalyzes the rapid photoinduced oxygenation of phosphites under mild conditions using aerial oxygen.

Scheme 1

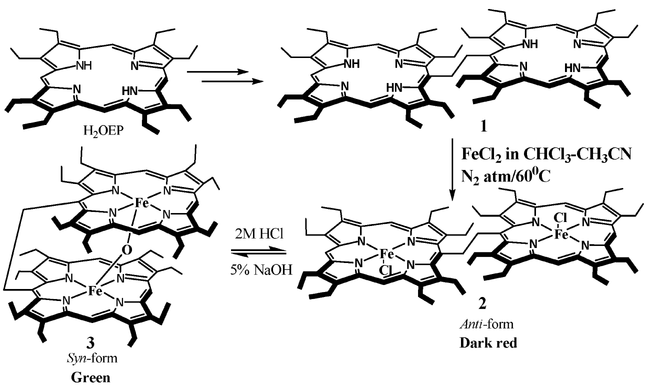

The chemistry of cofacial bisporphyrins is currently a topic of great interest, particularly because of their numerous applications in catalysis and photophysical properties.[1−7] The most successful cofacial bisporphyrin systems studied to date appear to be related to the so-called “Pac-Man” effect and have drawn considerable interest because of their small-molecule reactivity.[1−3] In this regard, the reactivity of photoactive iron bisporphyrins is of recent interest,[2,3] owing to the ability of these systems to utilize molecular oxygen for substrate oxidations via the formation of diiron(III) μ-oxobisporphyrins. The cofacial bisporphyrins with significant vertical flexibility are particularly effective at enhancing oxidation owing to greater substrate access for activation and subsequent reaction.[1−7] Herein we present the ferric complexes of highly flexible ethane-linked octaethylbisporphyrin, which authenticates the unprecedented ability to “open” and “close” its binding pockets with very high vertical flexibility in a single molecular framework as shown in Scheme 1.

The reaction of **1** with FeCl$_2$ under a N$_2$ atmosphere yields the corresponding diiron(III) chloride complex, **2**.[7] Spectroscopic characterizations[7] confirm its existence as the anti form in solution. However, a dichloromethane solution of **2** while shaking with a 5% NaOH solution immediately changes color from dark red to green because of the formation of *syn*-diiron(III) μ-oxobisporphyrin, **3**, which is isolated in pure form in excellent yields and structurally characterized (see the Supporting Information for details and, Figure S1 for the UV−vis spectrum). The facile syn−anti conformational switching has been found to be acid−base-controlled and reversible.

The complex **3** crystallizes as two different solvates: **3a** (·CH$_3$CN) and **3b** (·0.5toluene) grown from two different

---

* To whom correspondence should be addressed. E-mail: sprath@iitk.ac.in.

(1) Collman, J. P.; Wagenknecht, P. S.; Hutchison, J. E. *Angew. Chem., Int. Ed. Engl.* **1994**, *33*, 1537, and references cited therein.

(2) Harvey, P. D.; Stern, C.; Gros, C. P.; Guilard, R. *Coord. Chem. Rev.* **2007**, *251*, 401.

(3) Rosenthal, J.; Bachman, J.; Dempsey, J. L.; Esswein, A. J.; Gray, T. G.; Hodgkiss, J. M.; Manke, D. R.; Luckett, T. D.; Pistorio, B. J.; Veige, A. S.; Nocera, D. G. *Coord. Chem. Rev.* **2005**, *249*, 1316.

(4) (a) Clement, T. E.; Nurco, D. J.; Smith, K. M. *Inorg. Chem.* **1998**, *37*, 1150. (b) Senge, M. O.; Gerzevske, K. R.; Vicente, M. G. H.; Forsyth, T. P.; Smith, K. M. *Angew. Chem., Int. Ed. Engl.* **1993**, *32*, 750.

(5) (a) Chang, C. J.; Loh, Z.-H.; Shi, C.; Anson, F. C.; Nocera, D. G. *J. Am. Chem. Soc.* **2004**, *126*, 10013. (b) Deng, Y.; Chang, C. J.; Nocera, D. G. *J. Am. Chem. Soc.* **2000**, *122*, 410.

(6) (a) Borovkov, V. V.; Fujii, I.; Muranaka, A.; Hembury, G. A.; Tanaka, T.; Ceulemans, A.; Kobayashi, N.; Inoue, Y. *Angew. Chem., Int. Ed.* **2004**, *43*, 5481. (b) Hitchcock, P. B. *J. Chem. Soc., Dalton Trans.* **1983**, 2127.

(7) (a) Hembury, G. A.; Borovkov, V. V.; Lintuluoto, J. M.; Inoue, Y. *Chem. Lett.* **2003**, *32*, 428. (b) Borovkov, V. V.; Lintuluoto, J. M.; Inoue, Y. *Helv. Chim. Acta* **1999**, *82*, 919.

10.1021/ic801423g CCC: $40.75

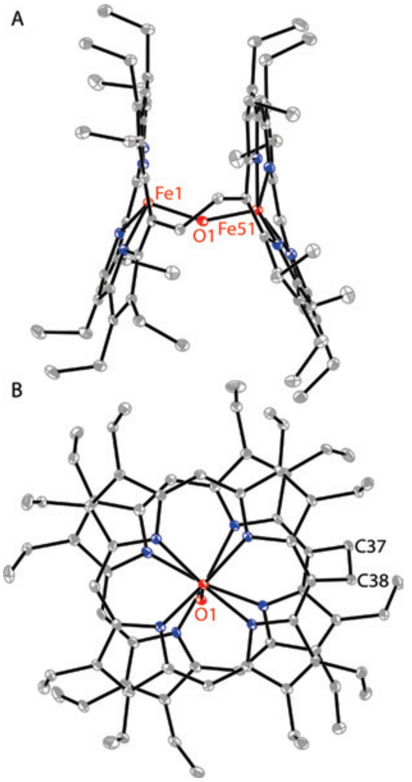

Figure 1. Two perspective views [A, side view; B, top view] of **3** showing 50% thermal contours for all non-hydrogen atoms. Selected bond distances (Å) and angles (deg) for **3a**: Fe1−O1, 1.779(2); Fe1−N1, 2.068(3); Fe1−N2, 2.060(3); Fe1−N3, 2.076(3); Fe1−N4, 2.069(3); Fe51−O1, 1.768(2); Fe51−N51, 2.075(3); Fe51−N52, 2.080(3); Fe51−N53, 2.069(3); Fe51−N54, 2.067(3); C37−C38, 1.546(5); Fe1−O1−Fe51, 147.9(1). Selected bond distances (Å) and angles (deg) for **3b**: Fe1−O1, 1.769(2); Fe1−N1, 2.081(3), Fe1−N2, 2.080(3); Fe1−N3, 2.073(3); Fe1−N4, 2.075(3); Fe51−O1, 1.766(2); Fe51−N51, 2.068(3); Fe51−N52, 2.070(3); Fe51−N53, 2.084(3); Fe51−N54, 2.077(3); C37−C38, 1.554(5); Fe1−O1−Fe51, 151.1(1).

Table 1. Selected Geometrical Parameters

	3a	**3b**	$[Fe(OEP)]_2O$[a] (monoclinic)
Fe−O [Å]	1.774(2)	1.767(2)	1.755(10)
Fe−Np [Å]	2.070(3)	2.076(3)	2.080(5)
Fe−O−Fe [deg]	147.9(1)	151.1(1)	176.2(2)
Δ_{24}^{Fe}[b] [Å]	0.57	0.54	0.54
interplanar angle[c] [deg]	25	21.2	2.7
Δ_{24}[d] [Å]	0.20	0.18	0.03
closest contact [Å]	3.016(5)[e]	3.042(5)[e]	4.47

[a] Taken from ref 9. [b] Displacement of iron from the least-squares plane of porphyrin (24 atom). [c] Angle between the two least-squares planes (24 atom). [d] Average displacement of atoms from the least-squares plane (24 atom). [e] Distance between two bridged meso carbons.

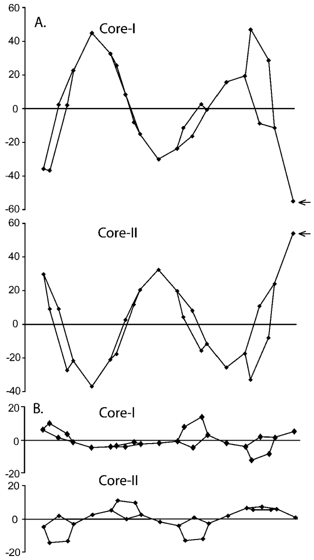

Figure 2. Out-of-plane displacements (in units of 0.01 Å) (A) for **3a** and (B) for $[Fe(OEP)]_2O$[9] (monoclinic) of the porphyrin core atoms from the mean porphyrin plane (24 atom). Arrows show the positions of the bridged meso carbons.

solvent combinations.[8] Both of them crystallize in a monoclinic crystal system with very similar structure and bonding parameters (Figure 1) in which the Fe···Fe distance is found to be 3.409(1) Å for **3a** [3.423(1) Å for **3b**]. However, there are only two structural reports so far with ethane-bridged bisporphyrin **1**; in one, it exists as the anti form with Ni···Ni separation of 9.93 Å, whereas the other stabilizes *tweezer*-type structures where the Zn···Zn separation is 5.604(5) Å.[6] A comparative structural analysis of *anti*-dinickel(II) porphyrin[6b] and *syn*-diiron(III) μ-oxobisporphyrin, **3**, has shown the unique ability of this platform to "open" and "close" its binding pocket with the highest vertical flexibility of over 6.5 Å reported to date.

Table 1 shows a comparison of the structures and geometrical features of **3** with the corresponding unbridged $[Fe(OEP)]_2O$.[9] The average Fe−O and Fe−N bond lengths in **3** are normal for any iron(III) μ-oxoporphyrin dimers.[9] The most striking feature of the structure is the small bent Fe−O−Fe angles of 147.9(1)° for **3a** [151.1(1)° for **3b**]. For comparison, the two smallest Fe−O−Fe angles reported so far for any cofacial bisporphyrinic μ-oxo dimers are one for a dibenzofuran-bridged cofacial bisporphyrin (158.7°) and another one for a diporphyrin xanthene methoxyaryl oxo-bridged dimer (155.2°).[5]

The close approach of the two porphyrin rings leads to a remarkable core deformation with an average deviation of 0.20 Å for **3a** (0.18 Å for **3b**) from the mean porphyrin plane, while the meso carbons that are connected through the bridging ligands are displaced the most (Figure 2). Two cores are structurally inequivalent (Figure 3) and are not parallel with respect to each other; in fact, half of the cores are nearly coplanar (dihedral angles of 5.3° and 5.6° for **3a** and **3b**, respectively), with ~3.7 Å separations allowing strong intramolecular $\pi-\pi$ interactions, while the other half make dihedral angles of 45.7° and 38.0° in **3a** and **3b**, respectively. The relative orientations between two porphyrin rings are such to make a tortional angle of 16.1° for **3a** (16.4° for **3b**), while the interplanar angle is 25° for **3a** (21.2° for **3b**).

---

(8) Crystal data for **3a**: monoclinic, space group *P*21/*n*, $a = 16.475(4)$ Å, $b = 15.317(3)$ Å, $c = 26.587(6)$ Å, $\beta = 96.988(4)°$, $V = 6659(3)$ Å^3, $Z = 4$, $D_c = 1.257$ Mg/m^3, $T = 100(2)$ K, no. of reflections used = 12 001, $\theta_{max} = 25.25°$, R1 = 0.066 [for $I > 2\sigma(I)$], wR2 (all data) = 0.1650, GOF on $F^2 = 0.986$. Crystal data for **3b**: monoclinic, space group *P*21/*n*, $a = 16.4668(8)$ Å, $b = 15.3828(7)$ Å, $c = 26.7700(13)$ Å, $\beta = 97.3970(10)°$, $V = 6724.6(6)$ Å^3, $Z = 4$, $D_c = 1.250$ Mg/m^3, $T = 100(2)$ K, $\theta_{max} = 25.50°$, R1 = 0.0593 [for $I > 2\sigma(I)$], wR2 (all data) = 0.1576, GOF on $F^2 = 1.033$.

(9) Cheng, B.; Hobbs, J. D.; Debrunner, P. G.; Erlebacher, J.; Shelnutt, J. A.; Scheidt, W. R. *Inorg. Chem.* **1995**, *34*, 102.

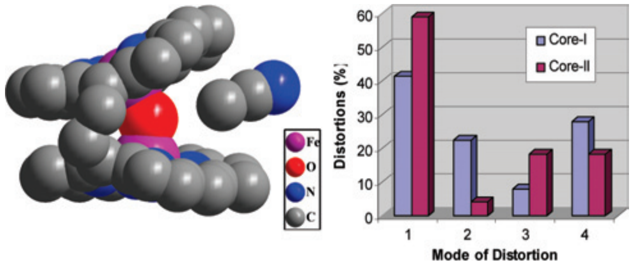

Figure 3. Diagram on the left showing the close contacts between two rings of **3a** and also the position of CH_3CN (hydrogen and ethyl groups are omitted for clarity). Histogram on the right showing the nature of the distortions (calculated using NSD program[10]) for two porphyrin cores in **3a**. Mode of distortions: 1, ruffle; 2, saddle; 3, dome; 4, wave.

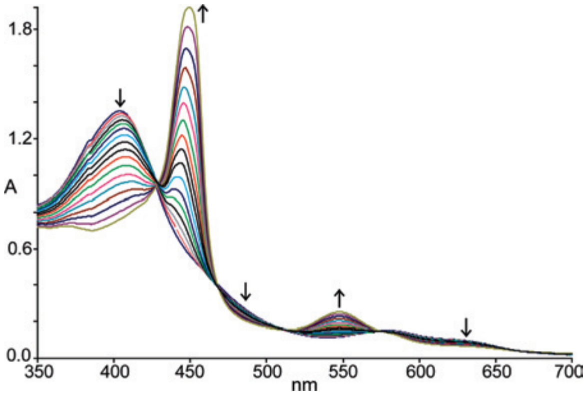

Figure 4. Time-evolution spectral changes for photolysis of benzene solutions of **3** ($\sim 10^{-6}$ M) in the presence of triethyl phosphite ($\sim$0.3 M) at 295 K under anaerobic conditions. The arrows indicate the disappearance of **3** and the appearance of a phosphite-bound diiron(II) bisporphyrin species. Spectra were recorded over the span of 2.5 h.

The closest intramolecular nonbonding C···C distance is between two bridging meso carbons with a separation of 3.016(5) Å for **3a** [3.042(5) Å for **3b**], which are well below the van der Waals radius of the atoms. There are at least five other C···C nonbonding distances (<3.4 Å) between two porphyrin rings that are also less than the van der Waals radius. The solvent molecules (CH_3CN for **3a** and toluene for **3b**) are wedged into the opening between two rings and are stabilized by attractive CH$-\pi$ and $\pi-\pi$ interactions with the rings (Figure 3). Similar stabilization of the substrates by the rings could be anticipated, which may be responsible for the selectivity and efficiency of the catalytic processes in the so-called “Pac-Man” systems.

Variable-temperature magnetic susceptibility measurements have been carried out for **3** between 5 and 350 K. The magnetic moments decrease from 2.65 μ_B at 350 K, with a decrease of the temperature, and reach a plateau at about 60 K, which is consistent for strongly antiferromagnetically coupled $S = {}^5/_2$ pairs. The $\chi_M T$ vs T data have been subjected to a least-squares fit ($-J$, 126.6 cm^{-1}) to the expression derived from the spin Hamiltonian $H = -2JS_1S_2$, where $S_1 = S_2 = {}^5/_2$. The cyclic voltammogram of **3** shows four reversible one-electron oxidations at 0.57, 0.87, 1.27, and 1.39 V and one reduction at -1.39 V (Figure S2 in the Supporting Information), whereas $[Fe(OEP)]_2O$ shows similar oxidations at relatively higher potentials (at 0.65, 0.93, 1.30, and 1.54 V) and reductions at slightly lower potential (-1.35 V) under identical conditions.

The complex **3** is very inert to $P(OR)_3$ (R = Me, Et); however, photoirradiation ($\lambda_{exc} > 365$ nm; O$-$Fe LMCT transition) in the presence of excess phosphite in a benzene solution under anaerobic conditions immediately changes their absorption spectra (Figure 4); a clean and quantitative photoreaction is evidenced by well-anchored isosbestic points. Moreover, each photoreaction yields a stoichiometric amount of $O{=}P(OR)_3$ and a single porphyrin product that is found to be a diiron(II) bisporphyrin complex with axial phosphite ligands, the electronic spectra (Figure S3 in the Supporting Information) of which are consistent with five-coordinate iron(II) species[11] and also show ^{31}P NMR signals at 11.4 and 7.4 ppm for R = Me and Et, respectively. Figure S4 (Supporting Information) shows the ^{1}H NMR spectrum of diiron(II) bisporphyrin generated in situ under N_2. However, the reaction of two separate ferrous porphyrin subunits with O_2 reforms **3** for re-entry into the catalytic cycle, which upon photoirradiation generates the highly oxidized ferryl intermediate ($PFe^{IV}{=}O$)[11] responsible for substrate oxidation.

In conclusion, we have presented here a remarkably bent diiron(III) μ-oxobisporphyrin containing a highly flexible ethane linker, which quickly “opens” and “closes” its binding pockets by manipulating the acidity/basicity of the solution, leading to facile syn$-$anti conformational switching with a very high vertical flexibility of over 6.5 Å in a single molecular framework. The structures of **3** provide the smallest known Fe$-$O$-$Fe angles for any iron(III) μ-oxo dimers of porphyrin derivatives reported so far, where the rings are not slipped but are face to face in a nearly eclipsed geometry and are placed so close that at least six carbon atoms from each of the porphyrin macrocycles are driven to be essentially less than the van der Waals contact. The facile syn$-$anti conformational switching is indicative of a small energy change, and an accessible pocket with minimized conformational energy would lower the transition state energy for substrate activation. The complex **3** catalyzes the rapid photoinduced oxygenation of phosphites in solution using aerial oxygen. Work is in progress.

Acknowledgment. We are thankful to the Department of Science and Technology, Government of India, for financial support. S.K.G. and R.P. thank CSIR, India, for a fellowship.

Supporting Information Available: Synthesis and characterization for **3**, UV$-$vis spectrum and cyclic voltammogram of **3** (Figures S1 and S2), UV$-$vis and ^{1}H NMR spectra of the iron(II) bisporphyrins (Figures S3 and S4), and X-ray crystallographic details in CIF format. This material is available free of charge via the Internet at http://pubs.acs.org.

IC801423G

---

(10) Jentzen, W.; Song, X.-Z.; Shelnett, J. A. *J. Phys. Chem. B* **1997**, *101*, 1684.

(11) (a) Chang, C. J.; Baker, E. A.; Pistorio, B. J.; Deng, Y.; Loh, Z.-H.; Miller, S. E.; Carpenter, S. D.; Nocera, D. G. *Inorg. Chem.* **2002**, *41*, 3102. (b) Hodgkiss, J. M.; Chang, C. J.; Pistorio, B. J.; Nocera, D. G. *Inorg. Chem.* **2003**, *42*, 8270.